

## Article

# Verification of a Simplified Design Method for Timber–Concrete Composite Structures with Metal Web Timber Joists

Agris Rogainis <sup>1,\*</sup>, Dmitrijs Serdjuks <sup>1,\*</sup>, Karina Buka-Vaivade <sup>1</sup>, Pavel Akishin <sup>2</sup>, Genadijs Sahmenko <sup>2</sup>, Elza Briuka <sup>1</sup> and Vjaceslavs Lapkovskis <sup>1</sup>

<sup>1</sup> Institute of Structural Engineering, Riga Technical University, LV-1048 Riga, Latvia; agris.rogainis@hotmail.lv (A.R.); karina.buka-vaivade@rtu.lv (K.B.-V.); briukab@gmail.com (E.B.); vjaceslavs.lapkovskis@rtu.lv (V.L.)

<sup>2</sup> Institute of Structures and Materials, Riga Technical University, LV-1048 Riga, Latvia; pavel.akisins@rtu.lv (P.A.); genadijs.sahmenko@rtu.lv (G.S.)

\* Correspondence: dmitrijs.serdjuks@rtu.lv

**Abstract:** This study presents a comprehensive analysis of a simplified design methodology for timber–concrete composite roof and floor structures employing metal web beams, also known as posi-joisted beams, easi-joist, or open web joists, validated through both laboratory experiments and finite element (FE) method analyses. The proposed method integrates the transformed section method and the  $\gamma$ -method, as outlined in Annex B of EN1995-1-1 for mechanically jointed beams. The investigation focuses on roof and floor structures featuring posi-joisted beams, oriented strand board (OSB) sheets connected by screws, and a layer of concrete bonded to the OSB sheets using epoxy glue and granite chips. Two groups, each consisting of four specimens, were prepared for the laboratory experiments. Each specimen comprised two posi-joisted beams, 1390 mm long, connected by OSB/3 boards measuring 400 mm in width and 18 mm in thickness. The beams had a cross-sectional depth of 253 mm, corresponding to beams of grade PS10, with top and bottom chords made from solid timber (95 mm  $\times$  65 mm). Bracing members with cross-sections of 100 mm  $\times$  45 mm were used to join the bottom chords of the beams. A layer of self-levelling mass SakretBAM, 50 mm thick, was bonded to the OSB/3 boards using SicaDur 31 epoxy glue and granite chips (16–32 mm). The specimens underwent three-point bending tests under static loads, and FE modelling, conducted using Ansys R2 2022 software, was employed for both experimental groups. A comparative analysis of results obtained from the simplified design method, FE simulations, and experimental data revealed that the simplified method accurately predicted maximum vertical displacements of the roof fragment, including posi-joisted beams, with precision up to 11.6% and 23.10% in the presence and absence of a concrete layer, respectively. The deviation between normal stresses in the chords of the beams obtained through the simplified method and FE modelling was found to be 7.69%. These findings demonstrate the effectiveness and reliability of the proposed design methodology for timber–concrete composite roofs with posi-joisted beams.

**Keywords:** simplified design method; transformed section method;  $\gamma$ -method; laboratory experiment; three-point bending; finite element analysis; load-carrying capacity; maximum vertical displacements; timber–concrete composite; stone chip method; posi-joisted beam; roof structures; floor structures; metal web joists



**Citation:** Rogainis, A.; Serdjuks, D.; Buka-Vaivade, K.; Akishin, P.; Sahmenko, G.; Briuka, E.; Lapkovskis, V. Verification of a Simplified Design Method for Timber–Concrete Composite Structures with Metal Web Timber Joists. *Appl. Sci.* **2024**, *14*, 1457. <https://doi.org/10.3390/app14041457>

Academic Editors: Monia Montorsi and Silvia Barbi

Received: 12 January 2024

Revised: 4 February 2024

Accepted: 8 February 2024

Published: 10 February 2024



**Copyright:** © 2024 by the authors. Licensee MDPI, Basel, Switzerland. This article is an open access article distributed under the terms and conditions of the Creative Commons Attribution (CC BY) license (<https://creativecommons.org/licenses/by/4.0/>).

## 1. Introduction

The construction industry ranks among the primary contributors to the significant global carbon footprint, heavily relying on non-renewable energy and emitting greenhouse gases. Accounting for approximately 40% of global energy consumption and contributing to 33% of greenhouse gas emissions, the construction industry, demands comprehensive measures to mitigate carbon emissions [1–4]. Addressing this challenge requires tailored

government policies, robust carbon emission analysis, and adopting sustainable materials. Carbon emissions analysis across the building life cycle revealed that the construction phase alone contributes to 20–50% of total carbon emissions [5]. Using timber-based structural products is currently regarded as an environmentally friendly choice, aligning with government sustainable development and climate change mitigation strategies. Timber is a practical alternative to traditional building materials, offering a high strength-to-weight ratio, low carbon footprint, renewable resource availability, and aesthetic appeal [6–9]. Ongoing efforts to optimise timber's structural efficacy are under way, expanding the application domains of timber-based structural products [10].

Each material possesses distinct advantages and disadvantages, and the practice of combining different materials in construction has a long history. The primary objective of blending materials and ensuring their composite action in structures is to enhance the final structure's characteristics [11–13]. This typically involves reducing overall weight, increasing stiffness and load-bearing capacity, and improving the aesthetic appeal of buildings. Steel–concrete pairs stand out as one of the most widely used combinations of materials [14]. In the realm of composite structures for roofs and floors, one study focused on a combination of cold-formed steel beams and timber panels [15]. Special adhesive compositions have proven effective in enhancing shear connection and stiffness, surpassing traditional steel options [16]. Notably, I-joists have gained popularity as engineered timber products for floor and roof assemblies in both residential and commercial settings [17].

The advancement of innovative solutions in the application of timber structures and elements in constructing multi-storey timber buildings has necessitated the development of novel composite structural materials for the walls and floor components of these structures [18].

In recent decades, timber–concrete composite (TCC) structures have gained prominence, especially in the construction of multi-storey timber buildings [19,20]. TCC structures contribute to creating rigid or semi-rigid joints, with connectors playing a crucial role in transferring shear between concrete slabs and timber beams [21,22]. Timber–concrete composites are instrumental in constructing structures that are challenging or impossible with timber alone [23,24]. A recent paper presents an analysis of the use of timber–concrete composite materials and monolithic slabs in residential buildings [25]. Cross-linking various types of timber-based materials has found widespread use in critical structural elements and structures [26].

Ongoing research on steel mesh structures in timber buildings is in an active stage of development and implementation [27]. Posi-joist elements, exemplified in this publication, are a noteworthy instance. Stability under vibration loads for floor structures created using metal web joists is extensively detailed in another study [28].

Metal-web beams represent shallow parallel-chord trusses where timber flanges are interconnected through a system of triangulation facilitated by steel webs [29]. Posi-joisted beams offer several advantages over alternative timber structures. They seamlessly blend the weight advantage of timber with the strength of the posi-strut steel web, enabling flooring and roofing solutions that cover substantially greater distances than other timber materials. This exceptional feature provides unmatched design versatility, making posi-joists suitable for various residential, industrial, and commercial applications. The ability to span large distances facilitates various internal room configurations within an external structure, presenting clear design advantages. Increased load-carrying capacity is achieved by adjusting the depth of the cross-section using the posi-strut steel web [30].

The lattice posi-strut steel web creates a service void for easy access during the installation and maintenance of services in the floor zone. It also allows for mechanical ventilation and heat recovery systems. Additional advantages of posi-joisted beams include a decreased assembling mass; improved quality due to fabrication in industrial conditions; a wide fixing surface, simplifying the installation of floor decks and ceilings; minimized shrinkage; exceptional sound performance; and significant fire resistance.

Combining timber–concrete composite structures with posi-joisted beams further enhances the benefits, leading to increased stiffness in floor and roof structures [31,32]. The available information on the design of roofs and floors with posi-joisted beams is currently limited and incomplete. Although timber–concrete composite roof and floor structures with posi-joisted beams can be designed using the finite element (FE) method, a simplified approach is necessary for determining the major dimensions of the considered structure. Thus, the objective of this study was to develop and validate a simplified method for designing timber–concrete composite roof and floor structures with posi-joisted beams.

## 2. Materials and Methods

### 2.1. Design Method for Timber–Concrete Composite Structure with Metal Web Timber Joists

A simplified method for designing timber–concrete composite roof and floor structures with posi-joists was derived based on the transformed section method and the  $\gamma$ -method outlined in Annex B of EN1995-1-1 for mechanically jointed beams [33–35], which showed promising results in the case of timber–concrete composite structures with cross-laminated timber panel [20]. To validate the developed design method, timber–concrete composite specimens (see Figure 1a) were prepared for laboratory testing. These specimens featured two posi-joisted beams joined by OSBs as top chords. A group of specimens without a concrete layer have been prepared to assess the increase in load-carrying capacity achieved by the addition of a concrete layer (see Figure 1b).



**Figure 1.** Considered specimens with posi-joisted beams: (a) with a concrete layer; (b) without a concrete layer.

The investigation focused on a structure featuring posi-joisted beams manufactured in accordance with SIA “MiTek Baltic” technology, OSB sheets attached to the beams with screws, and a layer of concrete bonded to the OSB sheets using epoxy glue and granite chips. This structure served as the object of study for describing the proposed method. The dimensions of the two groups of the investigated specimens are summarized in Figure 2.

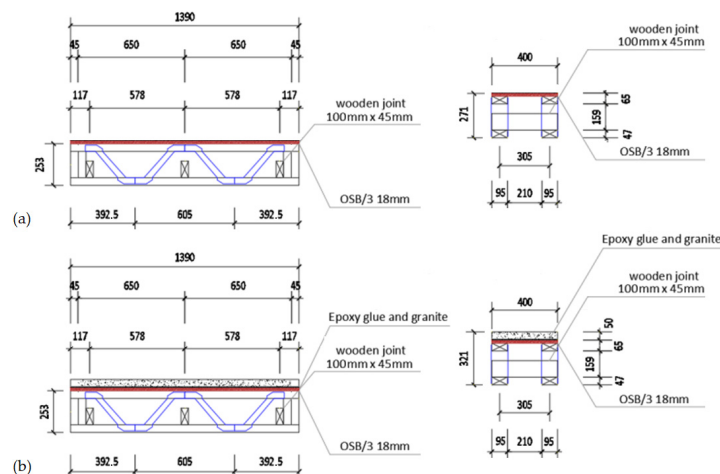


**Figure 2.** The investigated two groups of laboratory specimens: (a) without a concrete layer; (b) with an additional concrete layer; metal web is drawn in blue colour, top OSB sheet—in red colour.

The thickness of the concrete layer was chosen to ensure its operation primarily under compression, eliminating the need for principal reinforcement in the concrete layer. The analysis considered a segment of the structure consisting of two posi-joisted beams and corresponding layers of OSB and concrete.

The simplified method for designing a timber–concrete composite structure with posi-joisted beams comprises the following stages:

1. Choice of structural solution:

Selection of major geometric parameters, including the bay of the posi-joisted beams, depth of the beam cross-sections, thickness of the OSB decking, and thickness of the concrete layer. Recommendations from the existing literature [20,30] can guide this stage.

2. Determination of loads and actions and the formation of the design scheme:

Utilization of results from the first stage, considering climatic conditions, and applying recommendations [36] to establish a design scheme.

3. Global analysis and determination of internal forces:

Conducting global analysis to determine internal forces in all sub-members of the structure. For each posi-joisted beam, the uniformly distributed load on the beam can be replaced by an equivalent system of concentrated forces applied to the nodes of the top chord of the beam. Axial forces in the chords and lattice can be determined using structural mechanics methods.

4. Dimensioning of sub-members cross-sections:

Sizing the cross-sections of sub-members based on the internal forces identified in the global analysis, considering the requirements of Eurocode 2 for concrete layer, Eurocode 3 for steel web, and Eurocode 5 for timber elements.

5. Check of sub-members by ultimate limit state (ULS):

Verification of sub-members against the ultimate limit state (ULS).

6. Check of a fragment of the structure by serviceability limit state (SLS):

Examination of a fragment of the investigated structure to ensure compliance with the serviceability limit state (SLS).

Each stage builds upon the results of the previous one, providing a systematic approach to the design process for timber–concrete composite structures with posi-joisted beams.

The sizing of timber chords should adhere to strength conditions for the axially tensioned bottom chord and stability conditions for the axially compressed top chord [35]. It is crucial to consider existing recommendations [30] during this process.

The examination of the selected cross-sections of chords, determined in the previous stage, should be conducted using the transformed section method and the  $\gamma$ -method [33,35]. The cross-section of the analysed fragment of the structure was transformed into the timber of chords for this purpose (Figure 3).

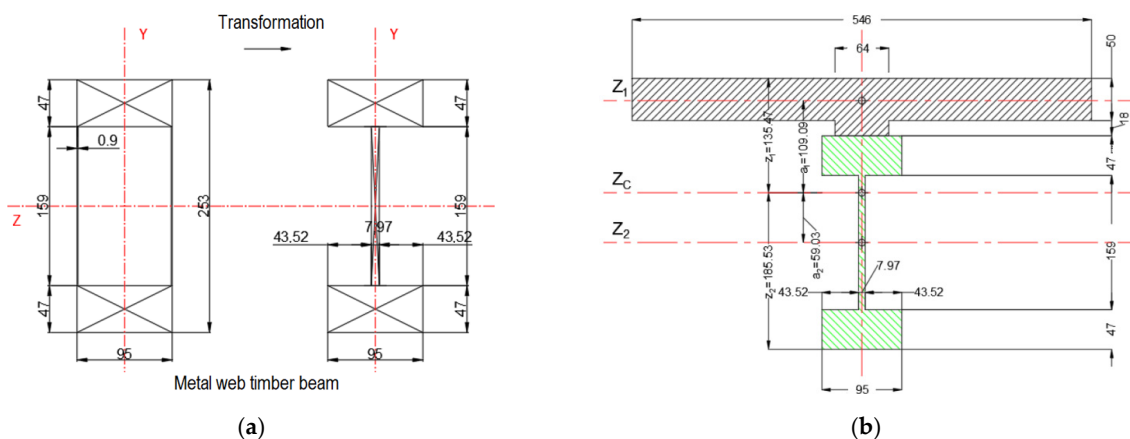


**Figure 3.** Transformed sections of (a) a posi-joisted beam and (b) a fragment of the timber–concrete composite structure with a posi-joisted beam.

The effective bending stiffness of the transformed section can be determined using Equation (1), outlined in Annex B of EN1995-1-1:

$$(EI)_{ef} = \sum_{i=1}^n \left( E_i \times I_i + \gamma_i \times E_i \times A_i \times a_i^2 \right) \quad (1)$$

where  $E_i$  is the mean value of modulus of elasticity of separate material layer, MPa;  $I_i$  is the moment of inertia of the separate layer relative to its own main axis, mm<sup>4</sup>;  $\gamma_i$  is the reduction factor, which takes into account compliance of the bonds;  $A_i$  is the cross-sectional area of the separate layer, mm<sup>2</sup>; and  $a_i$  is the distance from the neutral axis of the whole cross-section to the neutral axis of separate layer, mm.

Maximum normal stresses, acting at the chords of the posi-joisted beam, should be determined using Equation (2):

$$(\sigma)_{max} = \sigma_{global} + \sigma_{local} = \frac{M_d \times E_i}{(EI)_{ef}} \times (\gamma_i \times a_i + 0.5 \times h_i) \quad (2)$$

where  $M_d$  is the design value of bending moment, kNm;  $h_i$  is the height of the separate layer, mm.

Maximum shear stresses should be obtained using Equation (3):

$$\tau_{max} = \frac{V_d \times (ES)_{ef}}{(EI)_{ef} \times b} \quad (3)$$

where  $V_d$  is the design value of shear force, kN;  $b$  is the width of the separate layer, where shear stresses are calculated, mm; and  $(ES)_{ef}$  is the effective statical moment of the transformed section, which can be determined using Equation (4):

$$(ES)_{ef} = \sum_{i=1}^n \gamma_i \times E_i \times A_i \times a_i \quad (4)$$

The final stage of the method involves a check of the maximum vertical displacement, based on the effective bending stiffness determined using Equation (1). Maximum vertical displacements are calculated as the sum of the maximum vertical displacements due to the bending moment and the shear force.

## 2.2. Laboratory Experiment

A simplified method for designing timber–concrete composite roof and floor structures with posi-joisted beams underwent validation through a laboratory experiment [34]. To conduct this experiment, two groups of specimens were prepared, each comprising four specimens. The specimens in the first group consisted of two posi-joisted beams, each with a length of 1390 mm, joined by an oriented strand board (OSB/3) measuring 400 mm in width and 18 mm in thickness. The depth of the beams' cross-sections was set at 253 mm, aligning with beams of grade PS10 [30]. The top and bottom chords of the beams had equal cross-sections made from solid timber, measuring 95 mm × 65 mm. Additionally, three bracing members with cross-sections of 100 mm × 45 mm connected to the bottom chords of the beams.

The second group of specimens differed in terms of the addition of a 50 mm concrete layer, comprising self-levelling mass SakretBAM produced by SAKRET (Riga, Latvia). This layer was bonded with OSB/3 sheets using epoxy glue SicaDur 31 produced by Sika (Baar, Switzerland) and granite chips with a fraction size of 16–32 mm were incorporated. The dimensions of both types of the laboratory specimens are summarized in Figure 2. The production process of the specimens in the second group is illustrated in Figure 4.

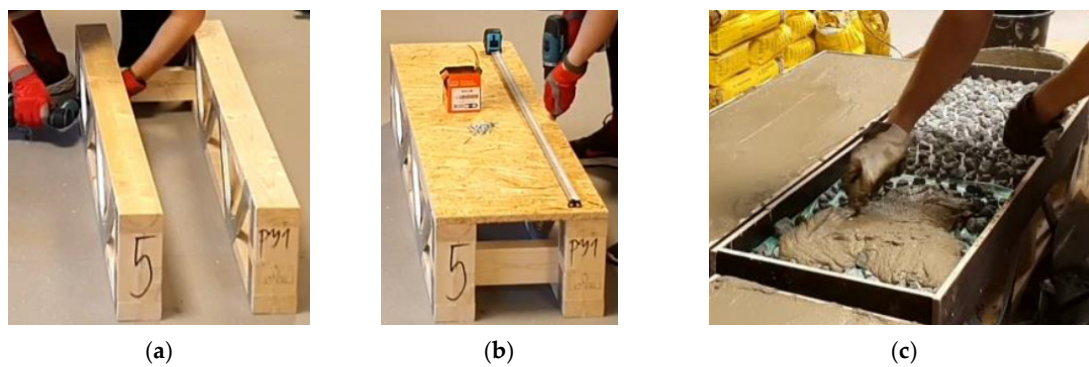


**Figure 4.** The process of the second groups specimens' development: (a) joining of the posi-joined beams with the bracing members; (b) joining of the posi-joined beams with the OSB/3 sheet and steel screws; (c) placement of the self-levelling mass, Sakret-BAM, on the OSB/3 surface, covered by the epoxy glue Sicadur 31 and granite chips.

The concrete underwent hardening over the course of one month from the placement moment. To prevent the development of shrinkage cracks, the surface of the concrete was covered with polyethylene foil. Subsequently, the moulds were removed, and both groups of specimens were subjected to testing until collapse under laboratory conditions.

Before the laboratory experiment, the load-carrying capacities and expected maximum vertical displacements for both groups of specimens were determined using the previously described simplified method for designing timber–concrete composite roof and floor structures with posi-joined beams, specifically for the case of three-point bending. The load-carrying capacities were found to be 24 kN for the first group and 46 kN for the second group. The experimental setup is illustrated in Figure 5 [34].

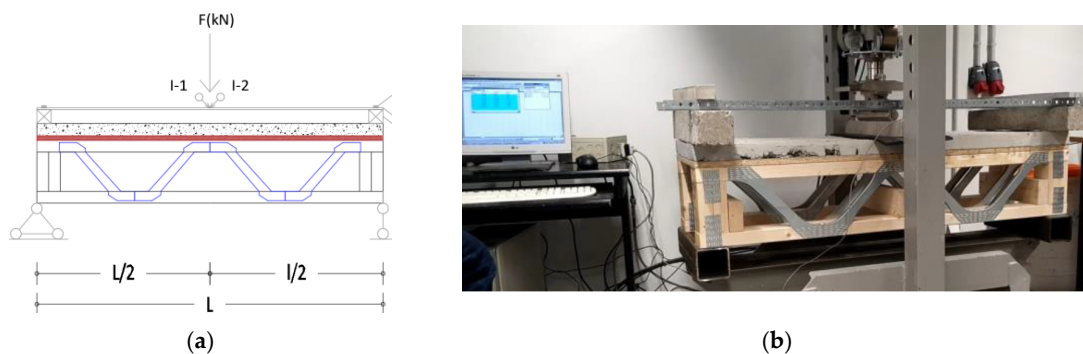


**Figure 5.** Scheme of laboratory experiment: (a) scheme of the specimen loading; (b) general view of the laboratory equipment during the testing of the specimen from the second group (with concrete).

Each specimen underwent three loading cycles until the load-carrying capacity of specimens without a concrete layer was reached, followed by loading until collapse. At each stage, the load increment was set at 3 kN, and the loading velocity did not exceed 2 kN/min. The results obtained for the first group of specimens are depicted in Figure 6.

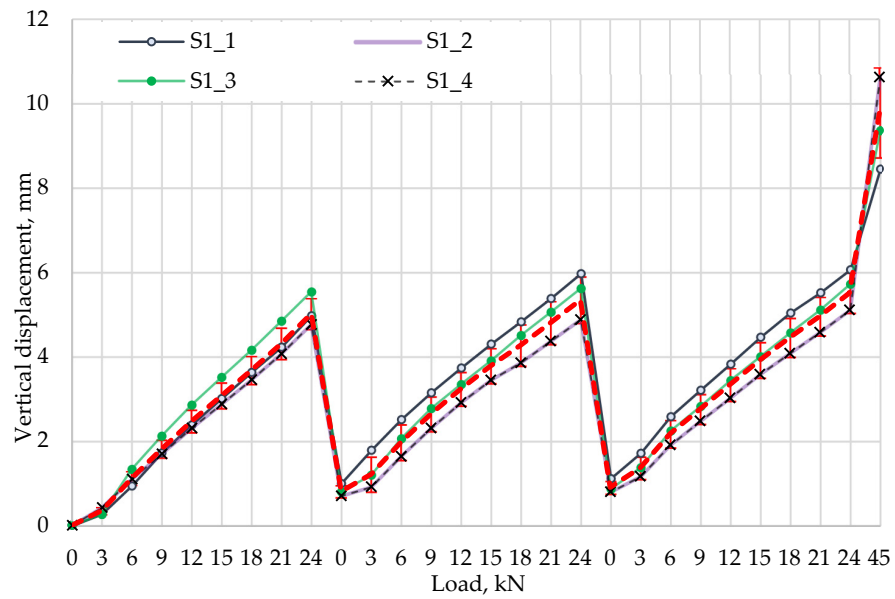


**Figure 6.** Maximum vertical displacement as a function of the applied load for specimens of the first group without a concrete layer (S1\_1, S1\_2, S1\_3, and S1\_4—four specimens of the first specimens’ group; S1\_mean—curve of the mean maximum vertical displacement with one standard deviation as a function of the applied load).

The experimentally obtained load-carrying capacities of the first group of specimens were 32.95 kN for the S1-1 specimen, 34.17 kN for specimen S1-2, 35.92 kN for specimen S1-3, and 35.47 kN for specimen S1-4. The mean value of the experimentally obtained load-carrying capacity was 34.63 kN. The maximum vertical displacements, when subjected to a design load of 24 kN, varied between 5.54 mm and 6.07 mm. When the load reached critical values, the maximum vertical displacements ranged from 8.45 mm to 10.63 mm.

The results for the second group of specimens are presented in Figure 7. Notably, the fourth specimen in the second group had a defect, and consequently, only three specimens from the second group were subjected to testing [34].

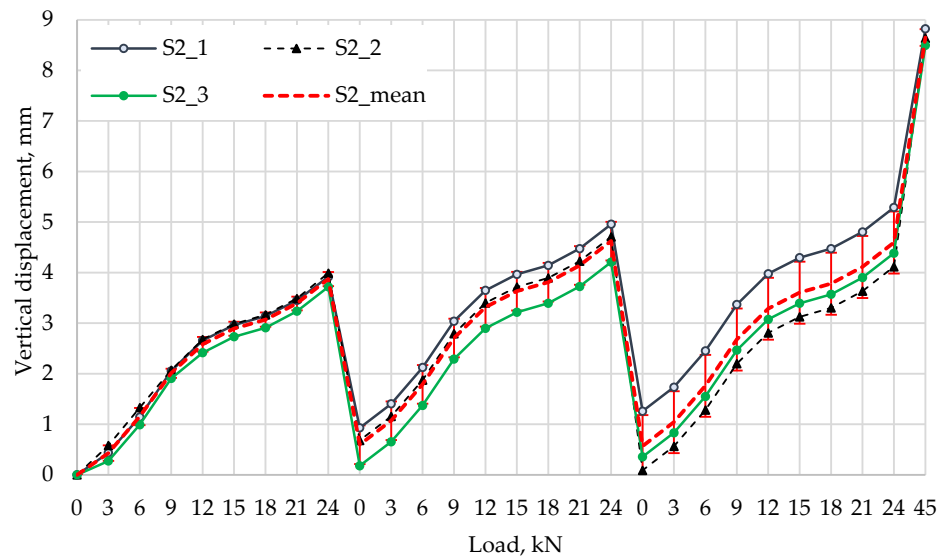


**Figure 7.** Maximum vertical displacement as a function of the applied load for the specimens of the second group with a concrete layer (S2\_1, S2\_2, and S2\_3—three specimens of the second specimens’ group; S2\_mean—curve of the mean maximum vertical displacement with one standard deviation as a function of the applied load).

The experimentally obtained load-carrying capacities of the second group of specimens were 46.69 kN for the S2-1 specimen, 45.35 kN for specimen S2-2, and 45.39 kN for specimen S2-3. The mean value of the experimentally obtained load-carrying capacity was 45.81 kN. The maximum vertical displacements, when subjected to a design load of 24 kN for the specimen with a concrete layer, varied between 3.89 mm and 5.29 mm. When the load reached critical values, the maximum vertical displacements ranged from 8.49 mm to 8.82 mm. The failure modes for specimens in both groups are illustrated in Figure 8.

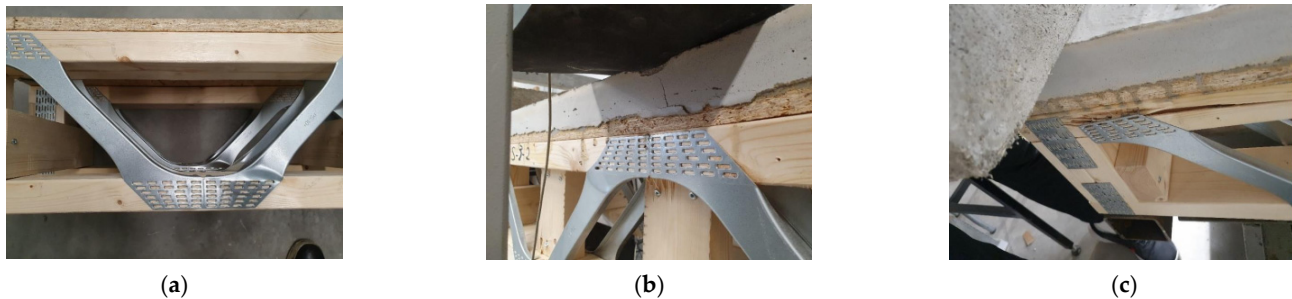


**Figure 8.** Modes of failure (a) for the S1 group specimens, (b,c) for the S2 group of specimens.

Local buckling of the steel webs was observed in all specimens of both the first and second groups (Figure 8a,b). Additionally, in the second group of specimens, extraction of the teeth in the steel-to-timber connection in the support zone on the top chord was noted (Figure 8c) [34].

### 2.3. FE Modelling

The finite element method, implemented using Ansys R2 2022 software, was employed for the FE modelling of both groups of the considered laboratory specimens to verify the efficacy of the proposed simplified method. The BEAM 188 element type was used to model timber chords, while the SHELL element type was utilized for modelling the OSB, concrete layer, and steel webs. Timber chords were represented as C24 class solid members with dimensions of 47 mm × 95 mm, and the steel braces, with punched steel plates having a cross-section of 47 mm × 1 mm, were made of S275 grade steel. All nodes were specified as rigid. The thicknesses of the OSB/3 and concrete layers were set at 18 mm and 50 mm, respectively, and the strength class of the concrete layer was designated as C25/30.

The FE models for the first and second groups of laboratory specimens, both without and with a concrete layer, are illustrated in Figure 9a,b, respectively.

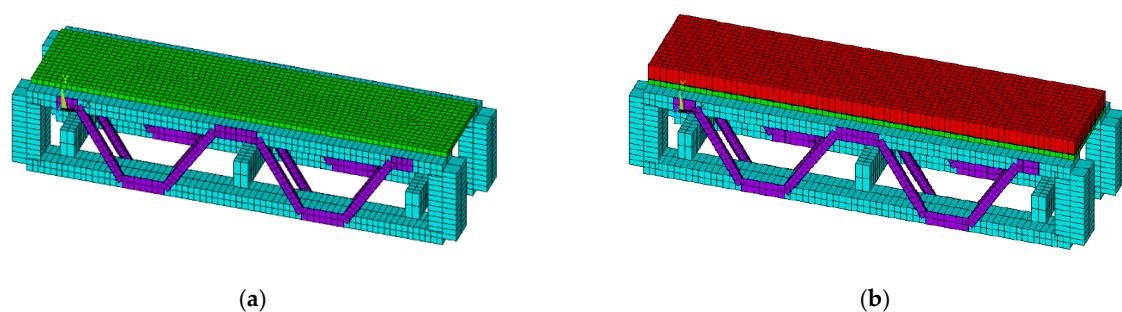


**Figure 9.** FE models of the first (a) and second (b) groups of laboratory specimens with and without concrete layer.

The developed FE models of the first and second groups of the laboratory specimens were analysed under the action of the concentrated 24 kN force through the scheme of three-point bending, as shown in Figure 5a. The value of the applied force was a design load for the specimen of the first group, determined by the simplified method, described in Section 2.1.

The results obtained for the second group of laboratory specimens using the developed FE model are presented in Figure 10. The potential for describing crack development was examined by utilizing the SOLID-FE-type to model the concrete layer for specimens of the second group.

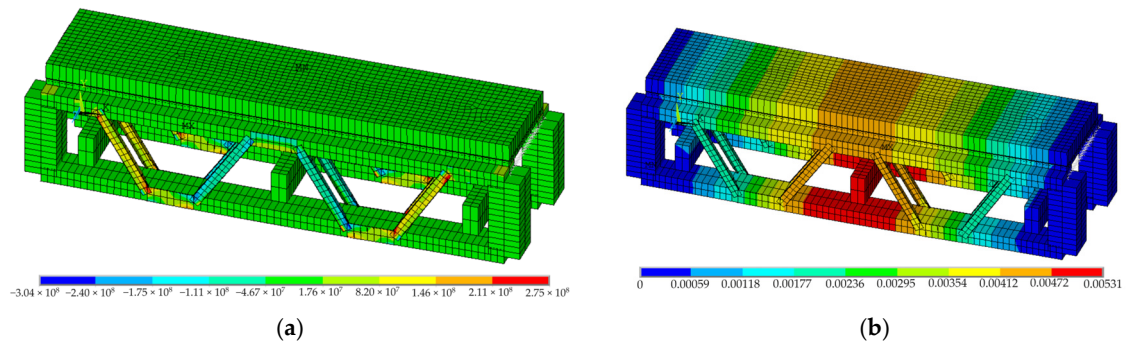


**Figure 10.** Stresses (a) and vertical displacements (b) obtained for the FE model of the second group of laboratory specimens with a concrete layer.

The scheme illustrating the development of cracks in the concrete layer and the vertical displacements obtained by the FE model, where the concrete layer was modelled using the SOLID-type finite element, is presented in Figure 11. Noteworthy is the absence of significant differences in the values of vertical displacements and stresses obtained by the models with SHELL and SOLID finite elements employed for modelling of the concrete layers.

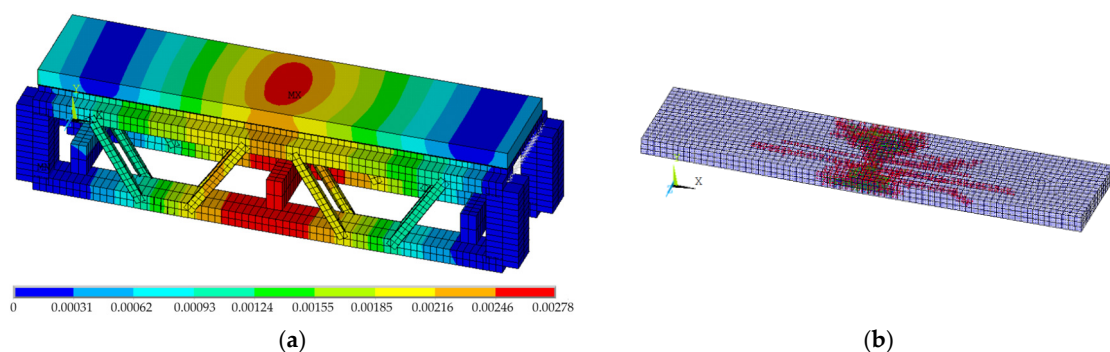


**Figure 11.** Vertical displacement (a) and the scheme of crack development (b), obtained for the FE model of the second group of laboratory specimens with a concrete layer.

### 3. Results and Discussions

The results obtained for both groups of specimens using the simplified design method, FE analysis, and laboratory experiments were consolidated and compared to validate the proposed simplified method. The focus was on evaluating the maximum vertical displacements and stresses acting in the chords of the posi-joisted beam. A graphical representation of the maximum vertical displacement as a function of the applied load for the first group of specimens is depicted in Figure 12. Notably, the OSB and steel lattice were modelled using the SHELL-type FE, as indicated in the description below Figure 12.

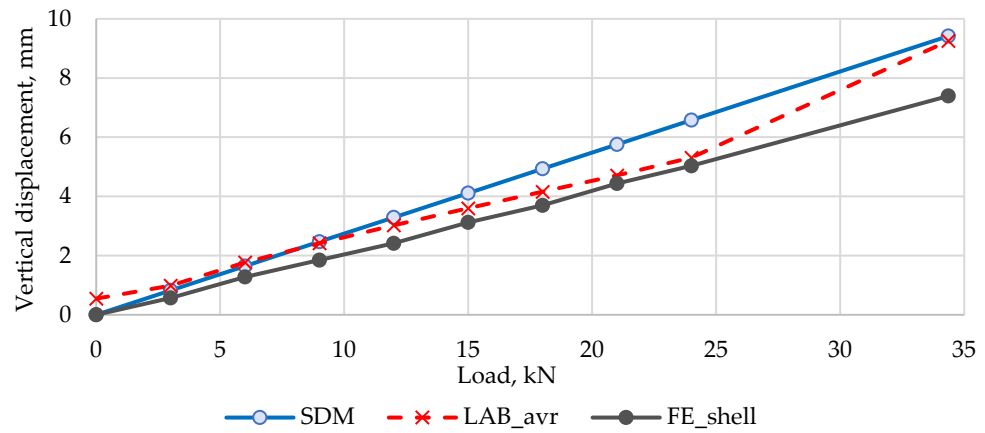


**Figure 12.** Maximum vertical displacement as a function of the applied load for specimens of the first group without concrete layer, by the simplified design method (SDM), FE analyses (FE\_shell), and laboratory experiments (LAB\_avr).

The obtained dependencies reveal that the average deflections from the experimental results initially surpassed those from theoretical calculations, attributed to residual deformations and creep effects. Beyond a load of 9 kN, the experimental displacement fell below the theoretical design curve. Throughout loading, the vertical displacement curve of the FE model remained consistently below the theoretical curve. The average difference between the results obtained by the simplified method and the experiment exceeded 23.10%. However, the difference between the results obtained by FE analysis and the experiment was more modest, at 6.25%.

For the first group of specimens, the maximum value of normal stresses obtained by the simplified method was 13 MPa, while the same value obtained by FE analysis was 12 MPa, resulting in a difference of 7.69%.

Similar results were obtained for the second group of specimens with the concrete layer (Figure 13). The chart with a line FE\_shell\_mod was derived from the FE model, where the OSB, concrete layer, and steel lattice were modelled by the SHELL-type finite element, taking into account the compliance of mechanical bonds (screws) between the top chord of the beam and the OSB layer.

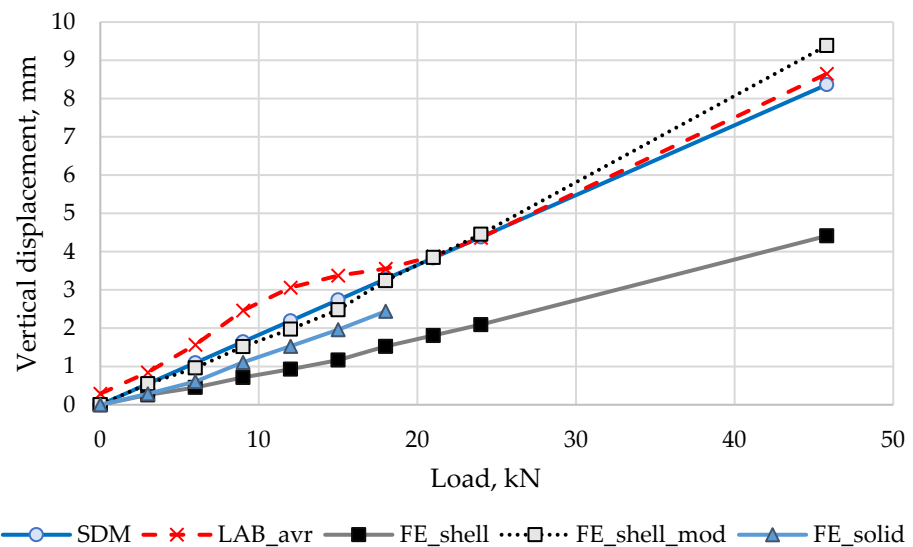


**Figure 13.** Maximum vertical displacement as a function of the applied load for the specimens of the second group (with concrete layer), by the simplified design method (SDM), FE analyses with three models (FE\_shell, FE\_shell\_mod, and FE\_solid), and laboratory experiments (LAB\_avr).

Bond compliance was assessed based on the experimental results and recommendations from the literature [35]. Comparison of the maximum vertical displacements obtained by the simplified design method and the aforementioned FE model indicated a mean difference of 6.40%. The differences for the FE models using the SOLID and SHELL types, without considering bond compliance, were significantly higher, reaching 63%. Comparing the maximum vertical displacements obtained by the simplified method and the experiment indicated a mean difference of 11.6% for the first loading cycle.

The chart shown in Figure 13, depicting the FE\_solid line, was generated by modelling the concrete layer using the finite element type SOLID. The chart is interrupted at a load level of 18 kN, where the development of the first cracks was noted. However, in practice, the failure of specimens was observed at an average load level of 45.81 kN for the three considered specimens. Therefore, it can be concluded that the use of the finite element type SOLID for modelling the concrete layer in timber–concrete composite structures with posi-joisted beams does not enable the accurate prediction of the structure’s behaviour at all loading stages. The SHELL type of FE is recommended for modelling the concrete layer, and compliance of the bonds should be considered in cases where mechanical fasteners are present between the layers of the considered structure.

Comparison of the results obtained by the simplified design method, FE model analyses, and experiments indicated that the simplified method accurately predicted the maximum vertical displacement for the investigated structure fragment, including posi-joisted beams, with precision values of 11.6% and 23.10% with and without a concrete layer, respectively. The difference in normal stresses in the chords of the beams obtained by the simplified method and the FEM model was 7.69%. This suggests that the generalized simplified method can be considered for the preliminary design and determination of structural parameters for developing FE models.

It can be concluded that the addition of a concrete layer with a thickness of 50 mm, possessing mechanical properties close to C25/30 strength class concrete, increases the load-carrying capacity of a structure with posi-joisted beams and OSB sheets joined with screws by 32.28%.

#### 4. Conclusions

In summary, a simplified method for designing timber–concrete composite roof and floor structures with posi-joisted beams was generalized and validated through laboratory experiments and FE model analysis. The method relies on the transformed section method and  $\gamma$ -method, and its applicability was tested on a structure comprising posi-joisted beams, OSB sheets joined with screws, and a layer of concrete bonded to the OSB sheets using epoxy glue and granite chips.

The findings indicate that the simplified method is suitable for preliminary design purposes of timber–concrete composite structures with posi-joisted beams and for determining structural parameters essential for developing FE models. A similar approach has previously been tested in the case of timber–concrete composite structures with cross-laminated timber panels, which highlights the potential versatility of suggested method across various configurations.

The mean difference in maximum vertical displacement between the simplified method and laboratory experiments did not exceed 11.6%. An FE model of the timber–concrete composite structure with posi-joisted beams, developed using Ansys R2 2022 software, was validated through laboratory experiments, with BEAM 188 and SHELL FE types recommended for modelling timber chords and OSBs, concrete layer, and steel webs, respectively.

Moreover, the addition of a concrete layer with a thickness of 50 mm and mechanical properties close to C25/30 strength class concrete resulted in a significant enhancement, increasing the load-carrying capacity of the investigated structure with posi-joisted beams, OSB sheets, and screws by 32.28%.

While the method exhibits promise as a preliminary design and parameter estimation tool, design practitioners should be aware of its limitations, particularly regarding loading conditions, material properties, and the absence of considerations for concrete creep and shrinkage effects. Further research is imperative to validate the method across a broader spectrum of conditions, enhancing its accuracy for practical design applications. The ongoing pursuit of validation with field data is crucial for bridging the gap between theoretical advancements and real-world structural behaviour. As long-term behaviour is essential, future research should incorporate extended experimental periods with the monitoring of structures over an extended period to gain insights into the effects of creep, shrinkage, and other time-dependent phenomena.

**Author Contributions:** Conceptualisation, A.R., D.S. and K.B.-V.; methodology, A.R., D.S., K.B.-V. and P.A.; software, P.A. and A.R.; investigation, A.R., D.S., G.S. and E.B.; data curation, A.R., D.S. and P.A.; writing—original draft preparation, D.S., K.B.-V. and V.L.; writing—review and editing, D.S., K.B.-V. and V.L.; visualisation, A.R. and K.B.-V.; project administration, D.S. and V.L. All authors have read and agreed to the published version of the manuscript.

**Funding:** This research was supported by the Latvian Council of Science funded project “Method of Correlation of Coaxial Accelerations in 6D Space for Quality Assessment of Structural Joints (COACCEL)” (Nr. lzp-2020/1-0240) and by “ZM-2024/9 Behaviour analyses of different types of timber–concrete beams type panels”.



**Institutional Review Board Statement:** Not applicable.

**Informed Consent Statement:** Not applicable.

**Data Availability Statement:** The data that support the findings of this study are available from the first author (A.R.) upon request.

**Conflicts of Interest:** The authors declare no conflicts of interest.

## References

1. Liu, T.; Chen, L.; Yang, M.; Sandanayake, M.; Miao, P.; Shi, Y.; Yap, P.-S. Sustainability Considerations of Green Buildings: A Detailed Overview on Current Advancements and Future Considerations. *Sustainability* **2022**, *14*, 14393. [\[CrossRef\]](#)
2. Basterra, L.-A.; Baño, V.; López, G.; Cabrera, G.; Vallelado-Cordobés, P. Identification and Trend Analysis of Multistorey Timber Buildings in the SUDOE Region. *Buildings* **2023**, *13*, 1501. [\[CrossRef\]](#)
3. Kiviste, M.; Musakka, S.; Ruus, A.; Vinha, J. A Review of Non-Residential Building Renovation and Improvement of Energy Efficiency: Office Buildings in Finland, Sweden, Norway, Denmark, and Germany. *Energies* **2023**, *16*, 4220. [\[CrossRef\]](#)
4. Sizirici, B.; Fseha, Y.; Cho, C.-S.; Yildiz, I.; Byon, Y.-J. A Review of Carbon Footprint Reduction in Construction Industry, from Design to Operation. *Materials* **2021**, *14*, 6094. [\[CrossRef\]](#)
5. Chen, L.; Huang, L.; Hua, J.; Chen, Z.; Wei, L.; Osman, A.I.; Fawzy, S.; Rooney, D.W.; Dong, L.; Yap, P.-S. Green Construction for Low-Carbon Cities: A Review. *Environ. Chem. Lett.* **2023**, *21*, 1627–1657. [\[CrossRef\]](#)
6. Bazli, M.; Heitzmann, M.; Ashrafi, H. Long-Span Timber Flooring Systems: A Systematic Review from Structural Performance and Design Considerations to Constructability and Sustainability Aspects. *J. Build. Eng.* **2022**, *48*, 103981. [\[CrossRef\]](#)
7. Kremer, P.; Symmons, M. Mass Timber Construction as an Alternative to Concrete and Steel in the Australia Building Industry: A PESTEL Evaluation of the Potential. *Int. Wood Prod. J.* **2015**, *6*, 138–147. [\[CrossRef\]](#)
8. Ramage, M.H.; BurrIDGE, H.; Busse-Wicher, M.; Fereday, G.; Reynolds, T.; Shah, D.U.; Wu, G.; Yu, L.; Fleming, P.; Densley-Tingley, D.; et al. The Wood from the Trees: The Use of Timber in Construction. *Renew. Sustain. Energy Rev.* **2017**, *68*, 333–359. [\[CrossRef\]](#)
9. Dukarska, D.; Mirski, R. Wood-Based Materials in Building. *Materials* **2023**, *16*, 2987. [\[CrossRef\]](#)
10. Korolkov, D.; Gravit, M.; Aleksandrovskiy, M. Estimation of the Residual Resource of Wooden Structures by Changing Geometric Parameters of the Cross-Section. *E3S Web Conf.* **2021**, *244*, 04010. [\[CrossRef\]](#)
11. Vijayakumar, R.; Pannirselvam, N. Behaviour of a New Type of Shear Connector for Steel-Concrete Composite Construction. *Mater. Today Proc.* **2021**, *40*, S154–S160. [\[CrossRef\]](#)
12. Adawi, A.; Youssef, M.A.; Meshaly, M.E. Experimental Investigation of the Composite Action between Hollowcore Slabs with Machine-Cast Finish and Concrete Topping. *Eng. Struct.* **2015**, *91*, 1–15. [\[CrossRef\]](#)

13. Al-Zaidee, S.; Al-Hasany, E. Finite Element Modeling and Parametric Study on Floor Steel Beam Concrete Slab System in Non-Composite Action. *J. Eng.* **2018**, *24*, 95. [[CrossRef](#)]
14. Ahmed, I.M.; Tsavdaridis, K.D. The Evolution of Composite Flooring Systems: Applications, Testing, Modelling and Eurocode Design Approaches. *J. Constr. Steel Res.* **2019**, *155*, 286–300. [[CrossRef](#)]
15. Kyvelou, P.; Gardner, L.; Nethercot, D.A. Testing and Analysis of Composite Cold-Formed Steel and Wood-Based Flooring Systems. *J. Struct. Eng.* **2017**, *143*, 04017146. [[CrossRef](#)]
16. Marques, A.C.; Mocanu, A.; Tomić, N.Z.; Balos, S.; Stammen, E.; Lundevall, A.; Abrahami, S.T.; Günther, R.; de Kok, J.M.M.; Teixeira de Freitas, S. Review on Adhesives and Surface Treatments for Structural Applications: Recent Developments on Sustainability and Implementation for Metal and Composite Substrates. *Materials* **2020**, *13*, 5590. [[CrossRef](#)] [[PubMed](#)]
17. Harte, A.M.; Baylor, G.; O’Ceallaigh, C. Evaluation of the Mechanical Behaviour of Novel Latticed LVL-Webbed Joists. *Open Constr. Build. Technol. J.* **2019**, *13*, 1–13. [[CrossRef](#)]
18. Premrov, M.; Žegarac Leskovar, V. Innovative Structural Systems for Timber Buildings: A Comprehensive Review of Contemporary Solutions. *Buildings* **2023**, *13*, 1820. [[CrossRef](#)]
19. Estévez-Cimadevila, J.; Martín-Gutiérrez, E.; Suárez-Riestra, F.; Otero-Chans, D.; Vázquez-Rodríguez, J.A. Timber-Concrete Composite Structural Flooring System. *J. Build. Eng.* **2022**, *49*, 104078. [[CrossRef](#)]
20. Buka-Vaivade, K.; Serdjuks, D. Behavior of Timber-Concrete Composite with Defects in Adhesive Connection. *Procedia Struct. Integr.* **2022**, *37*, 563–569. [[CrossRef](#)]
21. Deam, B.L.; Fragiaco, M.; Buchanan, A.H. Connections for Composite Concrete Slab and LVL Flooring Systems. *Mater. Struct.* **2008**, *41*, 495–507. [[CrossRef](#)]
22. Buka-Vaivade, K.; Serdjuks, D.; Podkoritovs, A.; Pakrastins, L.; Mironovs, V. Rigid connection with granite chips in the timber-concrete composite. *Environ. Technol. Resour.* **2021**, *3*, 36–39. [[CrossRef](#)]
23. Dias, A.; Skinner, J.; Crews, K.; Tannert, T. Timber-Concrete-Composites Increasing the Use of Timber in Construction. *Eur. J. Wood Prod.* **2016**, *74*, 443–451. [[CrossRef](#)]
24. Buka-Vaivade, K.; Serdjuks, D.; Pakrastins, L. Cost Factor Analysis for Timber-Concrete Composite with a Lightweight Plywood Rib Floor Panel. *Buildings* **2022**, *12*, 761. [[CrossRef](#)]
25. Andaque, H.; Sadeghi, K. Comparison Between Timber Concrete Composite Slab and Solid Slab for Residential Buildings. *Int. J. Innov. Sci. Res. Technol.* **2023**, *8*, 612–623. [[CrossRef](#)]
26. Winandy, J.E.; Morrell, J.J. Improving the Utility, Performance, and Durability of Wood- and Bio-Based Composites. *Ann. For. Sci.* **2017**, *74*, 25. [[CrossRef](#)]
27. Bonde, A.; Karlsson, V. *Tillämpning av Posi-Joist i Större Byggnader*; Uppsala Universitet: Uppsala, Sweden, 2023.
28. Zhang, B.; Kermani, A.; Fillingham, T. Vibrational Performance of Timber Floors Constructed with Metal Web Joists. *Eng. Struct.* **2013**, *56*, 1321–1334. [[CrossRef](#)]
29. European Assessment Document–EAD 130031-00-0304. Metal Web Beams and Columns 2018. Available online: [https://www.eota.eu/download?file=/2014/14-13-0031/for%20ojeu/ead%20130031-00-0304\\_ojeu2019.pdf](https://www.eota.eu/download?file=/2014/14-13-0031/for%20ojeu/ead%20130031-00-0304_ojeu2019.pdf) (accessed on 13 December 2023).
30. Posi-Joist Brochure. *MiTek UK and Ireland*. Available online: <https://cdn.mitekea.com/wp-content/uploads/sites/23/2018/10/18094543/Posi-Joist-Brochure-.pdf> (accessed on 13 December 2023).
31. Robinsons, H.; Azmi, M.H.; Famijs, E.H. Composite Open-Web Joists with Formed Metal Floor. *Can. J. Civ. Eng.* **1978**, *5*, 1–10. [[CrossRef](#)]
32. Zhang, B.; Kermani, A.; Fillingham, T. Vibrations of Metal Web Joist Timber Floors with Strongbacks. *Proc. Inst. Civ. Eng.-Struct. Build.* **2016**, *169*, 549–562. [[CrossRef](#)]
33. Buka-Vaivade, K.; Serdjuks, D.; Goremikins, V.; Vilguts, A.; Pakrastins, L. Experimental Verification of Design Procedure for Elements from Cross-Laminated Timber. *Procedia Eng.* **2017**, *172*, 1212–1219. [[CrossRef](#)]
34. Rogainis, A. Design Methodology Analyse of Timber Concrete Roof with Parallel-Chord Trusses with Steel Lattice. Master’s Thesis, RTU, Riga, Latvia, 2023.
35. *EN 1995-1-1:2004+A 1*; Eurocode 5: Design of Timber Structures—Part 1-1: General–Common Rules and Rules for Buildings. European Committee for Standardization: Brussels, Belgium, 2008.
36. *EN 1991-1-1:2002 (E)*; Eurocode 1: Actions on Structures—Part 1-1: General Actions–Densities, Self-Weight, Imposed Loads for Buildings. European Committee for Standardization: Brussels, Belgium, 2002.

**Disclaimer/Publisher’s Note:** The statements, opinions and data contained in all publications are solely those of the individual author(s) and contributor(s) and not of MDPI and/or the editor(s). MDPI and/or the editor(s) disclaim responsibility for any injury to people or property resulting from any ideas, methods, instructions or products referred to in the content.